Available online at www.sciencedirect.com
SCIENCE DIRECT®
Journal of Nuclear Materials 353 (2006) 35–41
journal of nuclear materials
www.elsevier.com/locate/jnucmat

Thermal diffusivity and thermal conductivity of thoria–lanthana solid solutions up to 10 mol.% $LaO_{1.5}$

Dheeraj Jain [a], C.G.S. Pillai [a,*], B.S. Rao [b], R.V. Kulkarni [b], E. Ramdasan [b], K.C. Sahoo [b]

[a] *Chemistry Division, Bhabha Atomic Research Centre, Mumbai 400 085, India*
[b] *Post Irradiation Examination Division, Bhabha Atomic Research Centre, Mumbai 400 085, India*

Received 13 January 2006; accepted 17 February 2006

Abstract

A series of thorium oxide–lanthanum oxide solid solutions has been prepared by solid-state reaction. The phase behavior of thoria doped lanthanum oxide has been ascertained by X-ray diffraction technique. A complete solid solubility of $LaO_{1.5}$ up to 30 mol.% has been observed. Thermal diffusivity of a range of thoria–lanthana solid solutions has been measured in the compositional range from pure thoria to 10 mol.% $LaO_{1.5}$ by the laser flash method covering a temperature range from 373 to 1773 K. Thermal conductivity values have been calculated from measured diffusivity, density and specific heats of these solid solutions. An attempt has also been made to delineate a suitable mechanism for heat conduction in these solid solutions with the help of the standard phonon conduction equation for dielectric materials.

1. Introduction

Thermal conductivity studies of actinide-oxide based ceramics are important in respect to their application in nuclear technology. Apart from understanding the heat transport mechanism in these materials, thermal conductivity data of these oxide fuels and their solid solutions/composites with different fission products are essential for evaluating the fuel performance, developing and investigating a range of nuclear reactor fuels and is a much needed input for developing the simulation codes for the fuel performance in the reactor.

Rare earth elements, which constitute a major share of the fission products during fuel irradiation, are formed as oxides and get dissolved in the fuel matrix to form solid solutions [1]. In addition, these oxides are also used as fuel diluents, flux suppressors, neutron absorbers [2], materials for improved fuel–clad interaction resistance [3], etc. and hence augment the need for a systematic study of thermophysical properties of these fuel-rare earth oxide systems such as thermal conductivity, thermal expansion, etc. Numerous experimental and theoretical studies of an extensive nature have been reported on the thermal conductivity behavior of both irradiated as

* Corresponding author. Tel.: +91 22 2559 5355; fax: +91 22 2550 5151.
E-mail address: cgspil@apsara.barc.ernet.in (C.G.S. Pillai).

0022-3115/$ - see front matter © 2006 Elsevier B.V. All rights reserved.
doi:10.1016/j.jnucmat.2006.02.084

well as non-irradiated urania, urania–plutonia [4–10] and their solid solutions with different rare earth fission products [11–14]. However, there are very few reports addressing the thermal conductivity of thoria related fuel materials involving their interaction with different rare earth fission products [15–17].

The thermal conductivity of thoria–lanthana solid solutions has been previously studied by Murthi et al. [17] from 573 to 1573 K for a compositional range from 0 to 30 mol.% $LaO_{1.5}$. In this paper much attention has not been given to the lower concentrations of lanthana, which is of more relevance to the development of simulation codes for reactor applications. In view of this, we have studied the thermal diffusivity and thermal conductivity behavior of thorium oxide–lanthanum oxide solid solutions in a wider temperature range from 350 to 1773 K with a compositional range from 0 to 10 mol.% $LaO_{1.5}$. Further it was worth considering to reinvestigate the phase behavior and solubility limits of the thoria–lanthana system via the solid state reaction route, since these limits have been found to depend upon the preparation method employed as reported in the literature [17,18]. Attempts have also been made to delineate a suitable mechanism for the heat conduction in these solid solutions with the help of the standard phonon conduction in dielectric materials.

2. Experimental

The samples used in the present study were prepared in our laboratory by the conventional solid-state reaction route. Thorium oxide (Nuclear grade) and lanthanum oxide powders, both of 99.9% purity, were used as such without further purification. Both the powders were heated at 1173 K for 16 h before weighing the powders for the sample preparation in order to remove any moisture content or adsorbed CO_2 gas due to alkaline nature of lanthanum oxide. Appropriate ratios of powders were mixed into different compositions, ranging from 1 to 35 mol.% $LaO_{1.5}$ and thoroughly ground mechanically. Pure thoria powder was also subjected to the same preparation cycle for the reference sample. The powders were pre-compacted into cylindrical pellets (10 mm diameter and 10–12 mm height) without any binder and crushed again to fine powder. The sequence of pre-compaction-grinding-compaction was repeated twice. The samples were then heated to 1223 K (5 K/min), held at that temperature for 24 h, slowly cooled to ambient temperature, crushed once again to fine powder and finally compacted by hydraulic press into cylindrical pellets (14.5 mm diameter, 2–2.5 mm height) at a pressure of 250 MPa. The pellets were heated up to 1273 K (5 K/min) and held for 16 h and further heated slowly up to 1773 K (2 K/min) for final sintering at this temperature for 6 h. All the heating was done in static air. The pellets were cooled slowly (3 K/min) to room temperature. All the samples were phase characterized by X-ray diffraction analysis using a powder diffractometer (Philips, Model PW 1820 controlled by PW 1710 micro-processor) with Ni-filtered Cu Kα (0.154 nm) radiation. Silicon was used as an external standard. The lattice parameters were determined by a least-squares refinement program. Bulk densities of the pellets were measured geometrically.

Thermal diffusivity measurements were carried out employing the laser flash technique [19,20]. The measurements were carried out using Flashline 2000 system (Anter Corporation) capable of measurements up to 2300 K. Cylindrical disc-shaped samples (12.7 mm diameter and approximately 2 mm thickness) were obtained from the sintered pellets by center-less grinding and polished from both the sides. The pellets were then cleaned ultrasonically in pure acetone for 30 min and dried thoroughly. In order to avoid any transmission of the laser beam through the samples, an opaque colloidal graphite suspension was sprayed over the front surface to give a thin coating of graphite. The rear surface of the pellets was also coated with a thin graphite layer to ensure uniform emissivity. These pellets were mounted in a molybdenum sample holder, which can carry six samples at a time. All measurements were carried out in flowing argon atmosphere, covering a temperature range from 373 to 1773 K. The samples were first heated to 1273 K (3 K/min) and cooled back slowly to room temperature in the flowing gas before starting the measurements to remove moisture or adsorbed CO_2, if at all present. All the thermal diffusivity measurements were found to be very well reproducible with the graphite standard (NIST) as well as our samples in the present investigations. The rear surface temperature–time profile of the samples was monitored by an indium antimonide infra-red detector and plotted online with the help of software.

3. Results and discussion

Fig. 1(a) presents the XRD patterns of all $Th_{1-x}La_xO_{2-\delta}$ samples (with $0 \leqslant x \leqslant 0.35$), indicating the

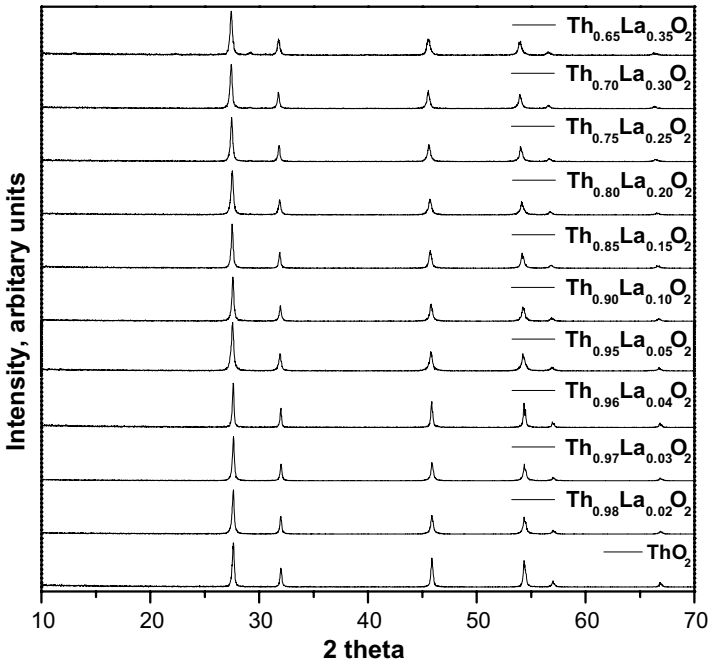

Fig. 1(a). X-ray powder diffraction pattern of all sintered samples.

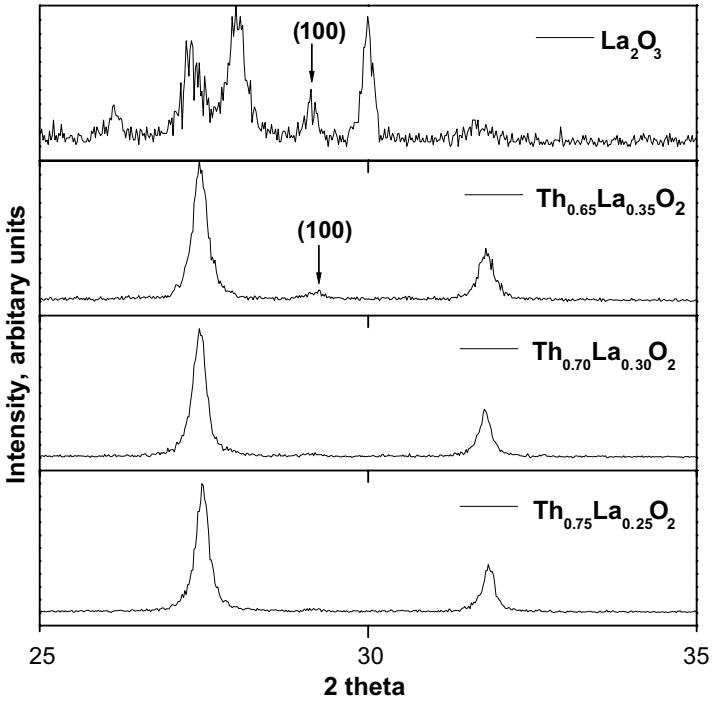

Fig. 1(b). Enlarged view of the XRD patterns along with the pure lanthana pattern.

formation of a single-phase fluorite-type solid solutions up to $x \leqslant 0.30$. However, as the lanthanum content exceeds this limit, an additional diffraction line corresponding to the (1 0 0) reflection of La_2O_3 [21] starts appearing in the XRD pattern, as indicated with the arrow in Fig. 1(b). Hence, we

conclude a solubility limit of approximately 30 mol.% $LaO_{1.5}$ in the thoria matrix via the solid-state reaction route. This limit is almost the same as the complete solubility region of $LaO_{1.5}$ in the ThO_2 matrix reported in the literature [17,22] and is in good agreement with the phase diagram of the system [22]. It is however much less than the recently reported solubility limit of 50 mol.% $LaO_{1.5}$ in thoria matrix by Panneerselvam et al. [18] for samples prepared by the co-precipitation method at relatively lower temperatures. This difference in the solubility and need for higher temperatures can be attributed to the limitations of the solid-state reaction methods over wet chemical approaches.

The lattice parameters calculated from the XRD data are found to increases with the La content 'x' and are given in Table 1. The least-squares fit of the data are very much near to the Vegard's law line, attesting the near stoichiometry of all the solid solutions. The empirical equation determined by this least-squares analysis is (a/nm = 0.558836 + 0.015747x), which is in good agreement with the previously reported values [23]. However, the variation in the linearity of the lattice parameter with increasing lanthana content can be due to the oxygen vacancies incorporated in the solid solutions due to the replacement of tetravalent thorium by trivalent lanthanum ions in the matrix. A positive shift in the d spacing for the 100% reflection line has been observed with increasing lanthana content up to 15 mol.% $LaO_{1.5}$ as shown in Fig. 2, which indicates a trend of lattice expansion due to guest atom incorporation at thorium sites. This has been further confirmed by the decreasing trend in the bulk density as well as theoretical density with increasing lanthana content as shown in Fig. 3. This increase in the lattice parameter with increasing La content is resulting from the larger ionic size of La^{+3} (0.116 nm) over Th^{+4} (0.105 nm) ions [24]. Bulk densities of

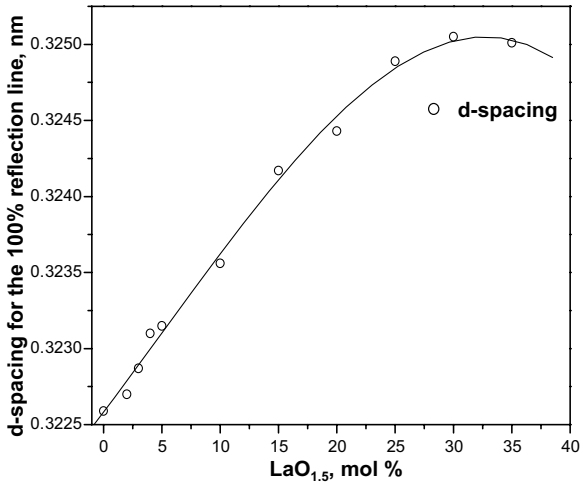

Fig. 2. Variation of d-spacing values of 100% reflection line with doped lanthana content.

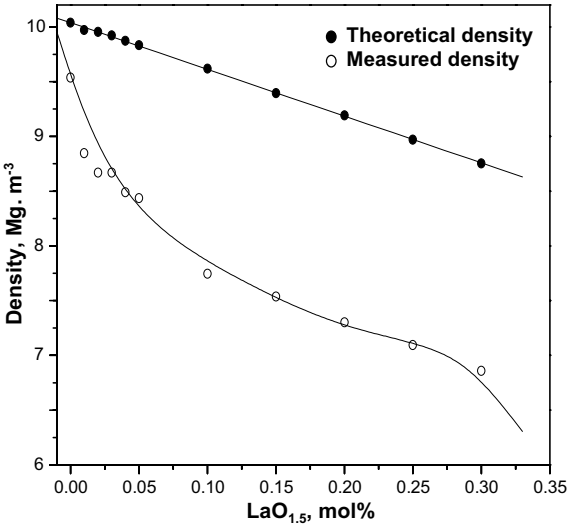

Fig. 3. Variation of both theoretical and observed values of bulk density with lanthana content at room temperature.

Table 1
Variation of lattice parameter and density of $Th_{1-x}La_xO_{2-\delta}$ samples

$LaO_{1.5}$ content (x in mol.%) $Th_{1-x}La_xO_{2-\delta}$	Lattice parameter (nm)	Bulk density (mg/m^3)	Theoretical density (mg/m^3)	Percent theoretical density
0.0	0.558971 ± 0.00015	9.538	10.040	95.01
0.01	0.559031 ± 0.00009	8.847	9.971	88.72
0.02	0.559252 ± 0.00007	8.671	9.954	87.10
0.03	0.559292 ± 0.00016	8.669	9.922	87.38
0.05	0.559519 ± 0.00008	8.435	9.834	85.77
0.10	0.560288 ± 0.00009	7.745	9.618	80.52
0.20	0.561822 ± 0.00012	7.302	9.191	79.44
0.30	0.563699 ± 0.00006	6.859	8.754	78.35

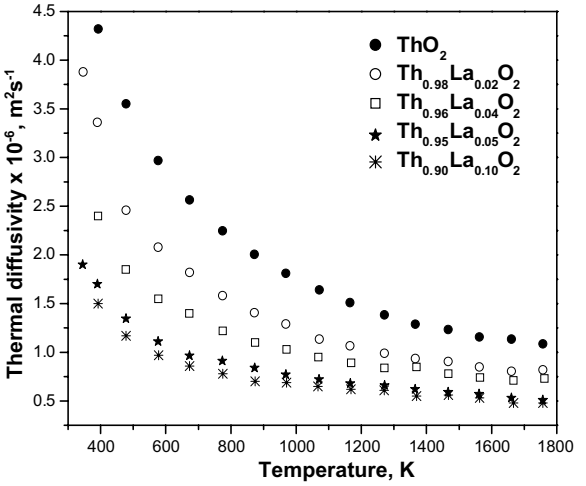

Fig. 4. Variation of as measured thermal diffusivity of $(Th_{1-x}La_x)O_{2-\delta}$ without porosity correction as a function of temperature and $LaO_{1.5}$ content.

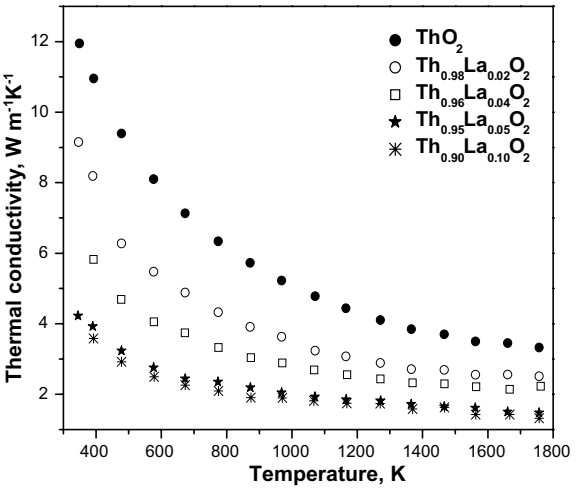

Fig. 5. Variation of thermal conductivity of $(Th_{1-x}La_x)O_{2-\delta}$ with temperature and $LaO_{1.5}$ content, after correction to 100% theoretical density.

all the samples were 83 ± 5% of the theoretical densities. The results of XRD analysis are summarized in Table 1.

Fig. 4 shows the variation of as measured thermal diffusivities, α (m^2/s) without any porosity correction of all $Th_{1-x}La_xO_{2-\delta}$ solid solutions with $0 \leqslant x \leqslant 0.10$ as a function of temperature, which was calculated from the following equation [19]:

$$\alpha = WL^2/t_{1/2}, \tag{1}$$

where W = heat loss parameter (0.1388), L = sample thickness and $t_{1/2}$ = time taken for half the maximum temperature rise of the rear surface. The value of W was in accordance with Clark and Taylor's method. All the thermal diffusivity measurements were found to be very well reproducible with the graphite standard (NIST) as well as our samples in the present investigations. A decrease in the thermal diffusivity was observed with increasing temperature for all the samples investigated. Moreover, an increase in $LaO_{1.5}$ content was also found to result in a decrease in the thermal diffusivity.

Thermal conductivities, λ (W/m/K) of all the samples were calculated from measured thermal diffusivities α, bulk densities ρ and specific heat capacities c_p of the solid solutions using Eq. (2) and are graphically shown in Fig. 5 as a function of temperature.

$$\lambda = \alpha\rho c_p. \tag{2}$$

It can be observed that addition of lanthana to the thoria matrix results in a systematic decrease in thermal conductivity at all the temperatures. Also, the conductivity decreases with increase of temperature for all these solid solutions studied. Due to the unavailability of the measured heat capacity data for the above solid solutions in literature, these values were estimated from the reported specific heat capacities [25] of individual components, viz., ThO_2 and $LaO_{1.5}$ and using the Neumann–Kopp's law:

$$c_p = \Sigma_n\{X_n(c_p)_n\}, \tag{3}$$

where X_n and $(c_p)_n$ are the mol fraction and individual molar specific heat capacity of component 'n', respectively. Thermal conductivity data for all the samples as presented in Fig. 5 were corrected for zero porosity using the following simplified equation [26].

$$\lambda = \lambda_0(1-P)^{2/3}, \tag{4}$$

where λ and λ_0 are the thermal conductivity of porous samples and theoretically dense samples, respectively, and P is the relative porosity calculated from the theoretical density (ρ_t) and measured density (ρ_m) as $P = \{\rho_t - \rho_m\}/\rho_m$. The correction for temperature dependence of density on the thermal conductivity data is not taken into account since the variations arising due to this are less than the accuracy limit of the measurement.

In order to compare our results with the appropriate theoretical models, it was considered better to study the thermal resistivity R (mK/W), reciprocal of the thermal conductivity as a function of

temperature and composition [2], which for a typical dielectric material can be given by the phonon conduction equation, Eq. (5):

$$1/\lambda = R = (A + BT), \tag{5}$$

where, 'A' corresponds to lattice defect thermal resistivity, arising from the scattering of phonons by lattice defects, impurities, isotopic or other mass differences as well as bulk defects such as grain boundaries in the samples, etc., while 'BT' is the intrinsic lattice thermal resistivity, arising from the phonon–phonon scattering interactions. Fig. 6 shows the variation of the thermal resistivity with temperature of the investigated samples. The linear variation of the observed resistivity with temperature for all the samples clearly shows that these samples behave like a typical dielectric material. The solid lines show the least-square fit of the experimental data with the values of the constants A and B, tabulated in Table 2.

It can be seen from the table that the constant 'A' increases with increasing lanthana content. An increase in the lanthana content results in more phonon defect centers in the media, due to both size and mass effect, and thereby resulting in additional strain in the lattice. Hence an increase in the defect thermal resistivity, i.e., 'A' is observed. It is also interesting to note that 'B' resulting from the intrinsic thermal resistivity, remains nearly the same for pure thoria as well as for the lanthana substituted thoria solid solutions up to 3 mol.% $LaO_{1.5}$, however, a slight increase is seen at higher doping concentrations. Similar results have been observed in the case of urania substituted thoria solid solutions [27], the reason for this behavior is explained therein. However, a slight increase in 'B' at higher doping levels can be justified on account of variations in the average molecular mass of the solid solutions.

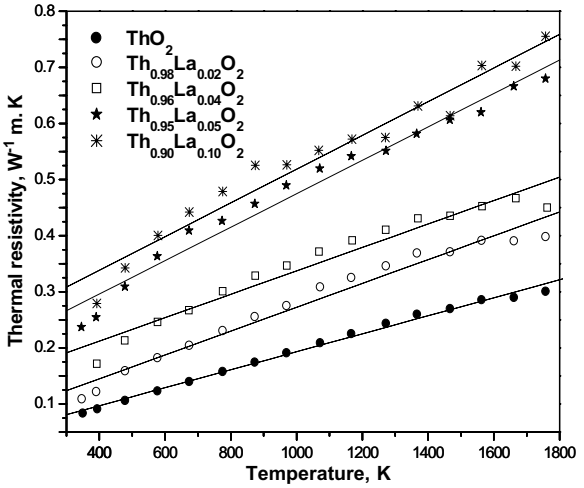

Fig. 6. Variation of thermal resistivity of $(Th_{1-x}La_x)O_{2-\delta}$ with temperature and $LaO_{1.5}$ content, after correction to 100% theoretical density.

Table 2
Values of coefficients A and B in $R = 1/\lambda = A + BT$ with lanthana content

$LaO_{1.5}$ (mol.%)	A (m/K/W)	B (m/W)
0.0	0.0327	0.0001603
0.02	0.0598	0.0002125
0.04	0.1285	0.0002087
0.05	0.1767	0.0002979
0.10	0.2179	0.0003005

4. Conclusions

The thermal conductivity of thorium oxide–lanthanum oxide solid solutions decreases with increasing lanthanum content and temperature. The variation of the thermal resistivity for the present system, obeys the standard phonon conduction equation found in dielectric materials. It can be inferred from the present results that doped lanthanum atoms serve as additional scattering centers for the phonons, whereas the intrinsic thermal resistivity remains almost unaffected by these foreign scattering centers.

Acknowledgements

The authors are grateful to Dr S. K. Kulshreshtha, Associate Director, Chemistry Group & Head, Chemistry Division for his keen interest and encouragement during the course of this work.

References

[1] H. Kleykamp, J. Nucl. Mater. 131 (1985) 221.
[2] W.K. Anderson, The Rare Earths, in: F. H. Spedding, A.H. Daane (Eds.), Robert E Krieger, Huntington, NY, 1971, p. 522.
[3] K. Bakker, H. Kwast, E.H.P. Cordfunke, J. Nucl. Mater. 226 (1995) 128.
[4] G.J. Hyland, J. Nucl. Mater. 113 (1983) 125.
[5] R.L. Gibby, J. Nucl. Mater. 38 (1971) 163.
[6] M. Amaya, T. Kubo, Y. Korei, J. Nucl. Sci. Tech. 33 (8) (1996) 636.
[7] Y. Philipponneau, J. Nucl. Mater. 188 (1992) 194.
[8] J.P. Moore, D.L. Mcelory, J. Am. Ceram. Soc. 54 (1971) 40.

[9] P.G. Lucuta, Hj. Matzke, I.J. Hastings, J. Nucl. Mater. 232 (1996) 166.
[10] C.G.S. Pillai, A.M. George, J. Nucl. Mater. 200 (1993) 78.
[11] K. Kurosaki, R. Ohshima, M. Uno, S. Yamanaka, K. Yamamoto, T. Namekawa, J. Nucl. Mater. 294 (2001) 193.
[12] S. Fukushima, T. Ohmichi, A. Maeda, M. Handa, J. Nucl. Mater. 115 (1983) 118.
[13] S.D. Preston, C. Barret, P. Fassina, K.C. Mills, N. Zaghini, High Temp. High Press. 21 (1989) 287.
[14] M. Amaya, M. Hirai, H. Sakurai, K. Ito, M. Sasaki, T. Namata, K. Kamimura, R. Iwasaki, J. Nucl. Mater. 300 (2000) 57.
[15] M. Murabayashi, J. Nucl. Sci. Tech. 7 (1970) 559.
[16] P.S. Murthi, C.K. Mathews, High Temp. High Press. 22 (1990) 379.
[17] P.S. Murthi, C.K. Mathews, J. Phys. D 24 (1991) 2202.
[18] G. Panneerselvam, M.P. Antony, T. Vasudevan, Mater. Lett. 58 (2004) 3192.
[19] W.J. Parker, R.J. Jenkins, C.P. Butler, G.L. Abbott, J. Appl. Phys. 32 (1961) 1679.
[20] R.E. Taylor, High Temp. High Press. 11 (1979) 43.
[21] JC-PDS card No: 05-0602.
[22] F. Sibieude, M. Foex, J. Nucl. Mater. 56 (1975) 229.
[23] A.M. Diness, RustomRoy, J. Mater. Sci. 4 (1969) 613.
[24] R.D. Shannon, Acta. Crystallogr. A 31 (1976) 751.
[25] I. Barin, O. Knacke (Eds.), Thermophysical Properties of Inorganic Substances, Springer-Verlag, Berlin, 1973, p. 574, 658.
[26] B. Schulz, High Temp. High Press. 13 (1981) 649.
[27] C.G.S. Pillai, P. Raj, J. Nucl. Mater. 277 (2000) 116.